

# Probing Columnar Discotic Liquid Crystals by EPR Spectroscopy with a Rigid-Core Nitroxide Spin Probe\*\*

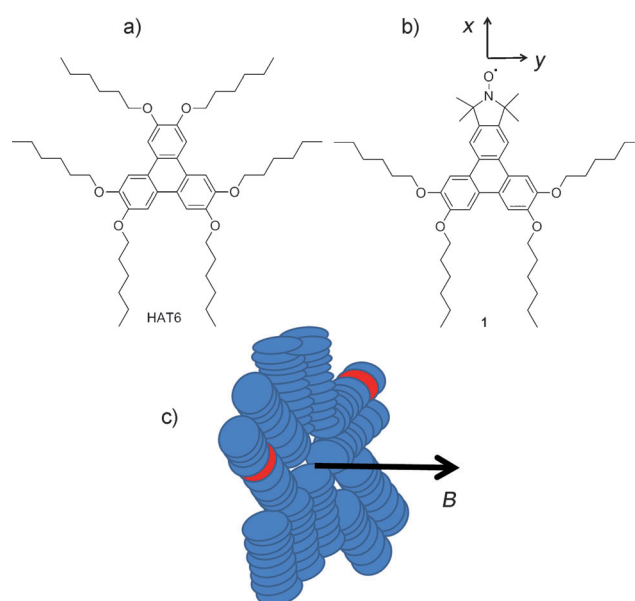
Hemant Gopee, Andrew N. Cammidge,\* and Vasily S. Oganessian\*

Within the last decade columnar discotic liquid crystals (DLCs) have attracted considerable interest, not least for their potential technological applications as one-dimensional conductors,<sup>[1]</sup> in sensors, field-effect transistors, and photovoltaic solar cells.<sup>[2–6]</sup> The coupling within stacked polyaromatic cores provides an efficient structure for charge transport along the columns thus providing one-dimensional pathways for charge and energy transfer with an efficiency that depends on the extent and stability of the overlap of the  $\pi$ -extended cores.<sup>[7]</sup> Understanding the dynamics and microscopic phase behavior of columnar discotics at the molecular scale is particularly challenging but fundamental for the link between new systems and devices with desired functionalities. The most extensively studied columnar LCs are based on hexasubstituted triphenylenes, of which hexakis(*n*-hexyloxy)-triphenylene (HAT6) is a representative example. HAT6 and other members of the HAT $n$  series have been studied by many methods including broad-band dielectric spectroscopy, DSC, X-ray diffraction, Muon spectroscopy, deuterium NMR spectroscopy, and quasi-electric neutron scattering.<sup>[8–11]</sup>

EPR spectroscopy of nitroxide spin probes (SPs) is a valuable method for the study of both structure and dynamics of complex partially disordered systems such as proteins and their complexes, DNA/RNA, biological membranes, nanoparticles, and soft matter.<sup>[12–22]</sup> EPR spectroscopy has the ability to resolve directly molecular re-orientational dynamics over time scales of  $10^{-11}$ – $10^{-7}$  s through the variation in spectral line shapes.<sup>[12]</sup> Because of the high sensitivity of the EPR technique only very low concentrations of the probe, about 100  $\mu$ M, are required experimentally so that the host system is essentially unperturbed. Continuous-wave (CW) EPR spectra provide three types of important information about the partially ordered fluid state, namely, molecular dynamics, local order of molecules averaged over a small volume, and global or long-range order in a multi-domain system. The spectra are very sensitive to changes in both dynamics (correlation times) and the order (order

parameter) of the SP within the LC system. For instance, rod-shaped EPR SPs such as cholestane derivatives have been successfully applied to study calamitic 4-*n*-alkyl-4'-cyanobiphenyl (nCB) nematic liquid crystals.<sup>[23–28]</sup> However, currently available spin probe molecules are incompatible with discotic systems.

Here we report the first application of EPR spectroscopy with a purpose-designed paramagnetic SP compatible with columnar discotic LCs. The SP design requires two important features. The probe itself should resemble the host matrix molecules as closely as possible to favour intercalation and cause minimal disruption to the phase, and the SP fragment itself must be orientationally rigid with respect to the discotic core. Discotic SP **1** was designed to meet these criteria and is shown in Scheme 1 together with HAT6. Its synthesis is shown in Scheme 2 and described in the Supporting Information.



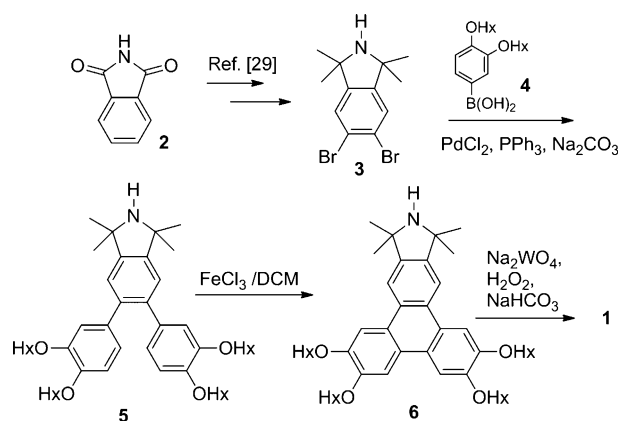
**Scheme 1.** a and b) Structures of HAT6 and the discotic rigid-core nitroxide spin probe **1**. Magnetic axes of the nitroxide head group are indicated by arrows, where *x* of the magnetic frame lies along the N–O direction and the *z* axis is perpendicular to the nitroxide plane. c) A schematic diagram of the columnar domain distribution of HAT6 molecules in the presence of a magnetic field, *B*. Spin probes are shown in red.

We demonstrate herein that the novel probe, when combined with variable-temperature CW EPR, is a sensitive reporter of the changes of molecular dynamics and order across the phase transitions in HAT6 thus allowing quantita-

[\*] Dr. H. Gopee, Prof. A. N. Cammidge, Dr. V. S. Oganessian  
School of Chemistry, University of East Anglia  
Norwich Research Park, Norwich, NR4 7TJ (UK)  
E-mail: a.cammidge@uea.ac.uk  
v.oganesyan@uea.ac.uk

[\*\*] V.S.O. thanks the EPSRC (grant number GR/H020411/1) for financial support of this work. We gratefully acknowledge further support from the Leverhulme Trust and the EPSRC Mass Spectrometry Service Centre (Swansea). We thank Prof. A. J. Thomson for helpful comments and discussions.

Supporting information for this article, including details of the EPR measurements and calculation of EPR spectra, is available on the WWW under <http://dx.doi.org/10.1002/anie.201303194>.



**Scheme 2.** Synthesis of the discotic spin probe **1** (Hx = *n*-C<sub>6</sub>H<sub>13</sub>).

tive determination of the order parameter, rotational correlation times, and columnar distribution in HAT6 at different temperatures. HAT6 can adopt three phases, namely, the isotropic (I), hexagonal columnar (Col) and crystalline (Cr), with temperatures of 373 and 335 K corresponding to I-Col and Col-Cr phase transitions, respectively.<sup>[10]</sup>

In DLCs molecular alignment occurs in macroscopic domains. Due to the large diamagnetic anisotropy of the polyaromatic core for most DLCs, including HAT6, the director (perpendicular to the aromatic planes, along the column axis) aligns normal to the applied magnetic field.<sup>[30]</sup> In the Col phase the magnitude of the resonant magnetic field of a  $g \approx 2$  paramagnet at X-band (9.5 GHz) of about 3400 G provides partial alignment of the columns of HAT6 as shown in Scheme 1c.

In a nitroxide SP the paramagnetic tensors  $\mathbf{g}$ , defining the interaction of the spin of the probe

with the external magnetic field, and  $\mathbf{A}$ , the <sup>14</sup>N nuclear hyperfine coupling to the electron spin, are both anisotropic leading to a strong dependence of the EPR resonances on the direction of the applied magnetic field relative to the principle magnetic axes. At X-band the spectrum is dominated by the anisotropic  $\mathbf{A}$  tensor resulting in three hyperfine coupling lines.<sup>[16,26]</sup> The EPR line shapes can range from three narrow lines due to averaging of the  $\mathbf{A}$  tensor in the case of fast isotropic motion to broad complex asymmetric features in the case of the so-called “rigid limit”. A variety of shapes can be observed between these two limiting cases depending on the level of motional constraint and the ratio between rotational correlation of the re-orientational dynamics of the SP and the hyperfine splitting.

Figure 1a and 1b show experimental EPR spectra at selected temperatures of HAT6 doped with the SP **1** measured on cooling across the I-Col and Col-Cr phase tran-

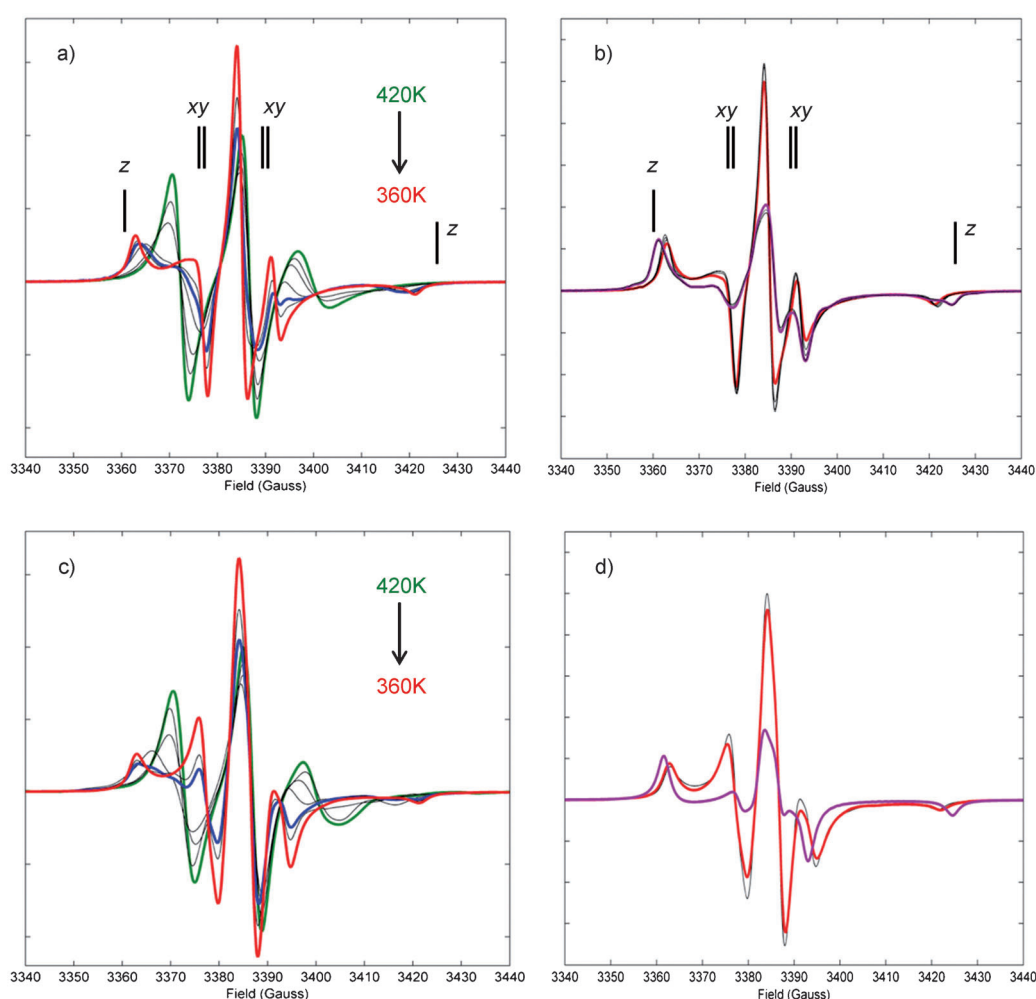


**Figure 1.** EPR spectra of HAT6 doped with the discotic rigid-core SP. The I phase at 420 K, Col phase at 360 K, and Cr phase at 320 K are shown as green, red, and purple lines, respectively. In panels (a) and (c) experimental and simulated spectra are shown at 420, 411, 399, 378, 372, 369, and 360 K representing most characteristic line shapes. The phase transition critical point is shown by blue lines. In panels (b) and (d) experimental and simulated EPR spectra are compared, respectively, across the Col-Cr phase transition. Overlapping black lines in (b) correspond to EPR spectra at several intermediate temperatures and a simulation for the Col phase at 339 K is shown by a black line in (d). Vertical lines in (a) and (b) indicate the resonance positions, which are inner and outer edges of left and right hyperfine coupling lines, corresponding to orientations of the magnetic field along *x*, *y*, and *z* axes of the SP.

sitions, respectively. A full set of EPR spectra measured every 3 K along with the integrated spectra are given in the Supporting Information in Figures S1–S4. For temperatures  $378\text{ K} < T < 420\text{ K}$  of the isotropic phase EPR spectra have characteristic line shapes corresponding to slow rotational diffusion motion. Upon approaching the critical point the spectra undergo dramatic change showing the emerging contribution from the Col phase in the sample. The line shape corresponding to a critical point at  $T = 372\text{ K}$  is shown by a blue line in Figure 1a. In the Col phase the magnetic field on average is lying in the plane of the nitroxide ring (see Scheme 1). As a result the line shape at 360 K of a pure Col phase is characterized by a substantial increase of the resonance intensity corresponding to the orientation of the magnetic field in the  $xy$  plane. For such orientations the distance between the resonance field positions (the inner edges of the hyperfine coupling lines shown as vertical lines in Figure 1a) approaches  $2A_{xx/yy}$  (about 12 G). The shift in intensity towards in-plane orientations of the field are particularly prominent in the EPR absorption profiles obtained by integrating the spectra (Figure S3).

Spectra measured upon further cooling of the sample through the Col-Cr phase transition are shown in Figure 1b. The Col-Cr transition is characterized by an abrupt change of the EPR lineshape which occurs within a narrow temperature interval ( $< 3\text{ K}$ ). This behavior is caused by the change in the molecular distribution upon going from Col (columnar) to powder Cr (random) when the number of resonances is decreased in the  $xy$  plane and increased in the  $z$  orientations (outer edges of the lines).

Figure 1c and 1d present EPR spectra calculated using a Brownian Dynamics (BD) simulation model for rotational diffusion of the SP in the presence of an ordering potential.<sup>[16,31,32]</sup> This model has been used here to simulate EPR line shapes corresponding to different phases of HAT6, namely, I, Col, and Cr. Isotropic contributions have been calculated as follows. First, two experimental EPR spectra at 420 and 399 K of purely isotropic phases were fitted by varying the adjustable parameters  $D_{x/y/z}^I$ , principle components of the rotational diffusion tensor of the probe. These temperatures and adjusted  $D_i^I$  values were then used as reference values to calculate the activation energy and temperature dependences of  $D_{x/y/z}^I$  according to the relationship  $D_i^I = A_i \exp(-E_i^I/kT)$ .<sup>[8,24]</sup> The isotropic contributions for the rest of the spectra shown in Figure 1b were subsequently predicted. Application of isotropic  $D_i^I$  proves inadequate to provide a satisfactory fit of the 420 K spectrum, particularly the intensity ratio between the low- and high-field hyperfine coupling lines. However, EPR spectra can be fitted well using the model of axial rotational diffusion. Parameters derived from the simulations are presented in Table 1. Overall, for isotropic states of HAT6 at temperatures  $< 420\text{ K}$  EPR spectra have characteristic line shapes corresponding to the slow motional regime of the axially symmetric rotational diffusion. Contributions in the EPR spectra from the columnar phase were simulated using a simple model of BD rotational diffusion of molecular disks in the presence of the axially symmetric ordering potential  $U(\theta(t)) = kTC_{20}(3\cos^2\theta(t) - 1)/2$ , the main axis of which is

**Table 1:** Parameters derived from the simulation and analysis of EPR lineshapes.

$T$ [K]	LC states	$D_{\parallel} [\text{s}^{-1}]/\tau_{\parallel} [\text{ns}]^{[a]}$	$D_{\perp} [\text{s}^{-1}]/\tau_{\perp} [\text{ns}]$	Contrib. [%]	$S$
420	I	1.60/6.22	5.80/1.72	100	0
411	I	1.32/7.52	4.68/2.13	100	0
399	I	1.02/9.77	3.60/2.77	100	0
378	I	0.62/16.10	2.18/4.57	100	0
372	I	0.53/18.80	1.86/5.35	50	0
	Col	0.85/11.70	2.23/4.48	50	0.78
369	I	0.49/20.11	1.34/5.75	40	0
	Col	0.81/12.34	2.22/4.50	60	0.79
360	Col	0.65/15.32	1.74/5.74	100	0.82
339	Col	0.20/45.00	0.47/21.07	100	0.83
320	Cr	0.12/80	0.12/80	100	0

[a]  $\tau_i$  are calculated using the relationship adapted for anisotropic diffusion  $\tau_i = 1/D_i$ .<sup>[33]</sup>

directed along the columnar director, where  $\theta$  is the angle between the  $z$  axis and director.<sup>[34]</sup> In addition, the effect of the director distribution of the columns was modelled using a normal distribution with a bandwidth of about  $42^\circ$ . This distribution is responsible for the spread of the observed resonances and, in particular, the positions of the outer edges of the left and right hyperfine coupling lines in Col. The best simulations were achieved with  $C_{20} = 3.00$  and the values for  $D_i^{\text{Col}}$  which are given in Table 1 along with corresponding correlation times and relevant values of the order parameter  $S$ . The adjusted values  $D_{\parallel}^{\text{Col}}$  and  $D_{\perp}^{\text{Col}}$  for the columnar phase are in good agreement with those previously reported<sup>[8]</sup> confirming that the tumbling motion of a disc is slightly faster than its spinning motion. Also the calculated value of the order parameter of the probe is in agreement with the columnar order parameter of the HAT6 molecule obtained from NMR studies.<sup>[8]</sup> A peak at about 3375 Gauss in the simulated Col EPR spectra appears to be stronger and narrower compared to the experimental one suggesting that a normal distribution of the director combined with the simple form of ordering potential employed by the model overestimate slightly the  $xy$ -plane resonances. Both  $D_i^{\text{Col}}$  and  $S$  indicate that the probe is a true mimic of HAT6 in terms of dynamics and order. Numerical analysis shows that the I-Col transition occurs in the  $369\text{ K} < T < 378\text{ K}$  temperature interval with the critical point at 372 K which has equal contributions from both phases of HAT6.

The line shape corresponding to a “powder” type distribution of Cr has been simulated using an even distribution of the molecules. The best fit is obtained using slow correlation times exceeding 80 ns which corresponds to the “rigid” limit in X-band EPR.

In addition, experimental line shapes corresponding to both the Col and Cr states of HAT6 show little dependence on the temperature at  $T < 360\text{ K}$  (Figure 1b and Figure S2). This is confirmed by the variation of the values of rotational diffusion coefficients in the simulation of Col EPR lineshapes. For instance, Figure 1d shows only a small difference between the simulated spectra corresponding to 360 and 339 K of Col phase although their relevant  $D_i^{\text{Col}}$  values differ by a factor of about 3.7.

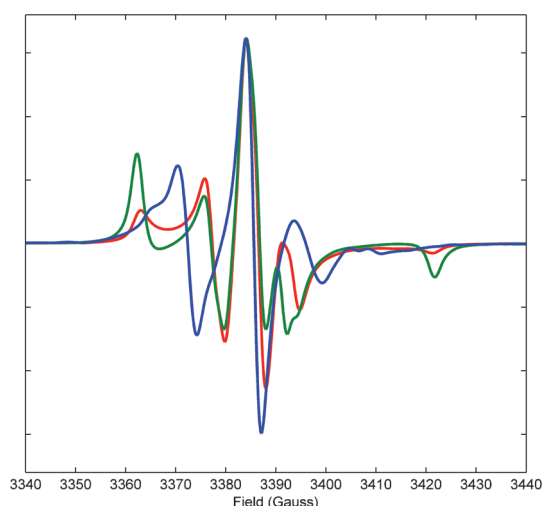


**Figure 2.** Comparison between EPR spectra simulated for the Col phase (red line) and when the director order was excluded (green line) and both the columnar director distribution and ordering potentials were excluded from the model (blue line).

To demonstrate the sensitivity of EPR spectral lineshapes to both the ordering potential for HAT6 molecules in the column and the director distribution of columns we have performed simulations of EPR lineshapes, shown in Figure 2, when the director order was excluded (even distribution of molecules; green line) and both director distribution and columnar ordering potential were excluded from the model (blue line). The resulting EPR spectra are compared in Figure 2 demonstrating that the columnar phase in HAT6 has significant impact on the EPR line shapes. In particular, resonances at  $z$  orientation are enhanced in the green curve, while in the blue curve the resonances corresponding to the orientation of the field along the nitroxide plane substantially diminish.

In conclusion, we have demonstrated the first application of EPR spectroscopy to the discotic columnar liquid crystal HAT6 using a rigid-core nitroxide SP designed and synthesized for this purpose. The probe intercalates within the columns of HAT6. EPR spectra measured at different temperatures across three phases show a strong sensitivity to the HAT6 phase composition, molecular rotational dynamics, and columnar order as well as the director distribution. Simulation of the EPR line shapes using a BD model gives a numerical estimate of these parameters at different temperatures along both I-Col and Col-Cr phase transitions. This study opens promising prospects for the application of EPR spectroscopy to a wide range of discotic LCs relevant to device applications, as well as to novel chromonic phases of discotic LCs for following their self-assembly in aqueous media.<sup>[35]</sup>

Received: April 16, 2013

Revised: June 25, 2013

Published online: July 19, 2013

**Keywords:** liquid crystals · EPR spectroscopy · molecular dynamics · phase transitions · spin probes

- [1] S. J. Woltman, G. D. Jay, G. P. Crawford, *Nat. Mater.* **2007**, 6, 929.
- [2] J. W. Goodby, *Chem. Soc. Rev.* **2007**, 36, 1855.
- [3] L. Schmidt-Mende, A. Fechtenkotter, K. Mullen, E. Moons, R. H. Friend, J. D. McKenzie, *Science* **2001**, 293, 1119.
- [4] F. C. Grozema, L. D. A. Siebbeles, *Int. Rev. Phys. Chem.* **2008**, 27, 87.
- [5] P. M. Prieto, *Opt. Express* **2004**, 12, 4059.
- [6] R. J. Bushby, K. Kawata, *Liq. Cryst.* **2011**, 38, 1415.
- [7] A. D. Ford, S. M. Morris, H. J. Coles, *Mater. Today* **2006**, 9, 36.
- [8] X. Shen, R. Y. Dong, N. Boden, R. J. Bushby, P. S. Martin, A. Wood, *J. Chem. Phys.* **1998**, 108, 4324.
- [9] F. M. Mulder, J. Stride, S. J. Picken, P. H. J. Kouwer, M. P. de Haas, L. D. A. Siebbeles, G. J. Kearley, *J. Am. Chem. Soc.* **2003**, 125, 3860.
- [10] Z. Yildirim, M. Wubbenhorst, E. Mendes, S. J. Picken, I. Paraschiv, A. T. M. Marceils, H. Zuilhof, E. J. R. Sudholter, *J. Non-Cryst. Solids* **2005**, 351, 2622.
- [11] I. McKenzie, A. N. Cammidge, H. Dilger, H. Gopee, R. Scheuermann, A. Stoykov, U. A. Jayasooriya, *Phys. Chem. Chem. Phys.* **2010**, 12, 9900.
- [12] L. J. Berliner, *Spin Labelling: The Next Millennium*, Plenum, New York, **1998**.
- [13] Z. F. Guo, D. Cascio, K. Hideg, W. L. Hubbell, *Protein Sci.* **2008**, 17, 228.
- [14] P. P. Borbat, A. J. Costa-Filho, K. A. Earle, J. K. Moscicki, J. H. Freed, *Science* **2001**, 291, 266.
- [15] G. Jeschke, *ChemPhysChem* **2002**, 3, 927.
- [16] H. J. Steinhoff, W. L. Hubbell, *Biophys. J.* **1996**, 71, 2201.
- [17] C. Beier, H. J. Steinhoff, *Biophys. J.* **2006**, 91, 2647.
- [18] M. Zerbetto, A. Polimeno, P. Cimino, V. Barone, *J. Chem. Phys.* **2008**, 128, 024501.
- [19] B. J. Gaffney, D. Marsh, *Proc. Natl. Acad. Sci. USA* **1998**, 95, 12940.
- [20] O. Schiemann, P. Cekan, D. Margraf, T. F. Prisner, S. Th. Sigurdsson, *Angew. Chem.* **2009**, 121, 3342; *Angew. Chem. Int. Ed.* **2009**, 48, 3292.
- [21] M. Zachary, V. Chechik, *Angew. Chem.* **2007**, 119, 3368; *Angew. Chem. Int. Ed.* **2007**, 46, 3304.
- [22] G. F. White, L. Ottignon, T. Georgiou, C. Kleanthous, G. R. Moore, A. J. Thomson, V. S. Oganessian, *J. Magn. Reson.* **2007**, 185, 191.
- [23] G. R. Luckhurst, *Thin Solid Films* **2006**, 509, 36.
- [24] R. Berardi, L. Muccioli, C. Zannoni, *ChemPhysChem* **2004**, 5, 104.
- [25] A. Arcioni, C. Bacchiocchi, I. Vecchi, G. Venditti, C. Zannoni, *Chem. Phys. Lett.* **2004**, 396, 433.
- [26] V. S. Oganessian, E. Kuprusevicius, H. Gopee, A. N. Cammidge, M. R. Wilson, *Phys. Rev. Lett.* **2009**, 102, 013005.
- [27] E. Kuprusevicius, R. Edge, H. Gopee, A. N. Cammidge, E. J. L. McInnes, M. R. Wilson, V. S. Oganessian, *Chem. Eur. J.* **2010**, 16, 11558.
- [28] F. Chami, M. R. Wilson, V. S. Oganessian, *Soft Matter* **2012**, 8, 6823.
- [29] A. S. Micallef, R. C. Bott, S. E. Bottle, G. Smith, J. M. White, K. Matsuda, H. Iwamura, *J. Chem. Soc. Perkin Trans. 2* **1999**, 65.
- [30] J.-H. Lee, S.-M. Choi, B. D. Pate, M. H. Chisholm, Y.-S. Han, *J. Mater. Chem.* **2006**, 16, 2785.
- [31] V. S. Oganessian, *J. Magn. Reson.* **2007**, 188, 196.
- [32] V. S. Oganessian, *Phys. Chem. Chem. Phys.* **2011**, 13, 4724.
- [33] R. J. Cherry, *Biochim. Biophys. Acta* **1979**, 559, 289.
- [34] E. Berggren, R. Tarroni, C. Zannoni, *J. Chem. Phys.* **1993**, 99, 6180.
- [35] J. Lydon, *J. Mater. Chem.* **2010**, 20, 10071.